



## 3D Gaussian descriptor: a new descriptor for 3D models

Mohamed Chaouch, Anne Verroust-Blondet

► **To cite this version:**

Mohamed Chaouch, Anne Verroust-Blondet. 3D Gaussian descriptor: a new descriptor for 3D models. IEEE International Conference on Multimedia and Expo 2009 (ICME 2009), Jun 2009, New-York, United States. pp.834-837, 2009, <10.1109/ICME.2009.5202624>. <hal-00802564>

**HAL Id: hal-00802564**

**<https://hal.inria.fr/hal-00802564>**

Submitted on 20 Mar 2013

**HAL** is a multi-disciplinary open access archive for the deposit and dissemination of scientific research documents, whether they are published or not. The documents may come from teaching and research institutions in France or abroad, or from public or private research centers.

L'archive ouverte pluridisciplinaire **HAL**, est destinée au dépôt et à la diffusion de documents scientifiques de niveau recherche, publiés ou non, émanant des établissements d'enseignement et de recherche français ou étrangers, des laboratoires publics ou privés.

# 3D GAUSSIAN DESCRIPTOR: A NEW DESCRIPTOR FOR 3D MODELS

Mohamed Chaouch and Anne Verroust-Blondet

INRIA Paris - Rocquencourt Domaine de Voluceau, B.P. 105 78153 Le Chesnay Cedex, FRANCE  
Email: {mohamed.chaouch, anne.verroust}@inria.fr

## ABSTRACT

This paper presents a new approach to 3D shape comparison and retrieval based on the computation of Gaussian transforms of the surface model on a set of points regularly distributed inside the model's bounding box. A study of the properties of the Gaussian term leads us to an efficient computation of the description. This method is evaluated on the Princeton Shape Benchmark database.

*Index Terms*— 3D shape retrieval, Gaussian transform

## 1. INTRODUCTION

The increasing number of available 3D shapes on the Internet or in domain specific databases motivated the need of content-based 3D retrieval systems. Numerous shape matching methods have been introduced (see a very good survey [1] and comparative studies of 3D retrieval algorithms [2, 3, 4, 5]). They can be split into two families: the 2D/3D approaches, where the model description is obtained through 2D projections of the 3D shape, and the 3D approaches. Some of the 3D methods are based on a partition of the enclosing space (partition into concentric shells and sectors around the model's centroid [6] or into voxels [7, 8]). In most of the case, a shape histogram describing either the volume or the surface of the 3D model is built and the comparison between two shapes is done using the  $L_1$  distance. Computing the distance between the histogram bins. In the case of the voxel-based approach proposed by Vranic [8], the 3D shape is represented by a volumetric data composed of a set of voxels or volume elements and the feature vector is a voxel grid.

Our descriptor uses a spatial decomposition of the 3D enclosing box upon where a description of the surface of the 3D model is built. To obtain a local description of the surface of the 3D shape, a 3D Gaussian function measuring the influence of the surface points on regularly spaced points is introduced. This constitutes the 3D Gaussian descriptor proposed in the next section. An efficient computation scheme is presented. The overall method is then evaluated on the Princeton Shape Benchmark.

## 2. 3D GAUSSIAN DESCRIPTOR

The *3D Gaussian Descriptor* (3DGD) of a model  $\mathcal{M}$  is a spatial description of  $\mathcal{M}$  built from the Gaussian law and obtained by a summation on the surface  $\mathfrak{S}$  of  $\mathcal{M}$ .

In the rest of the paper, a 3D model  $\mathcal{M}$  will be represented by its surface  $\mathfrak{S}$  composed of a set of triangular facets  $\{T_i\}_{i=1\dots N_T}$ .  $\mathcal{A}$  will denote the area of  $\mathfrak{S}$  and  $\mathcal{A}_i$  the area of the facet  $T_i$  for  $i = 1\dots N_T$ .

### 2.1. Definition

Let  $\sigma$  be a real number representing the width of a 3D volume defined around  $\mathfrak{S}$ . The Gaussian transform of the surface  $\mathfrak{S}$  on a point  $\mathbf{q}$  is:

$$g(\mathbf{q}, \mathfrak{S}, \sigma) = \iint_{\mathfrak{S}} e^{-d^2(\mathbf{p}, \mathbf{q})/\sigma^2} ds, \quad (1)$$

where  $d$  is the Euclidean distance from  $\mathbf{q}$  to the point  $\mathbf{p}$  of  $\mathfrak{S}$ . The Gaussian transform is used to build a description of  $\mathcal{M}$  on a set of points of the space as follows:

Let  $B$  be a bounding box of  $\mathcal{M}$ . It is a rectangular prism having the set of vertices  $(x, y, z)$  with  $x \in \{x_{min}, x_{max}\}$ ,  $y \in \{y_{min}, y_{max}\}$  and  $z \in \{z_{min}, z_{max}\}$ .  $B$  is subdivided into  $N^3$  rectangular cells having the  $\mathbf{q}_{ijk} = (x_i, y_j, z_k)$ ,  $i, j$  and  $k \in \{0, \dots, N-1\}$ , as centers:

$$x_i = x_{min} + (i + 0.5)\Delta_x, \quad \Delta_x = (x_{max} - x_{min})/N,$$
$$y_j = y_{min} + (j + 0.5)\Delta_y, \quad \Delta_y = (y_{max} - y_{min})/N,$$
$$z_k = z_{min} + (k + 0.5)\Delta_z, \quad \Delta_z = (z_{max} - z_{min})/N.$$

Then the 3D Gaussian descriptor is defined by  $\mathbf{G} = [g_{ijk}]$  with:

$$g_{ijk} = g(\mathbf{q}_{ijk}, \mathfrak{S}, \sigma) = \iint_{\mathfrak{S}} e^{-d^2(\mathbf{p}, \mathbf{q}_{ijk})/\sigma^2} ds, \quad (2)$$

where  $g_{ijk}$  is the local description of the surface  $\mathfrak{S}$  around  $\mathbf{q}_{ijk}$ . Let  $e_{ijk}^{\mathbf{p}}$  be the contribution of the point  $\mathbf{p}$  of  $\mathfrak{S}$  in the local description  $g_{ijk}$ . We have:

$$e_{ijk}^{\mathbf{p}} = e^{-d^2(\mathbf{p}, \mathbf{q}_{ijk})/\sigma^2} \quad (3)$$

In fact, the Gaussian transform amplifies the local influence of the surface. Let us consider the bunny model of Figure 1 (d). We see that the  $g_{ijk}$  are bigger around the extremities of the ears and of the legs, i.e. the regions of high presence of bunny's surface.

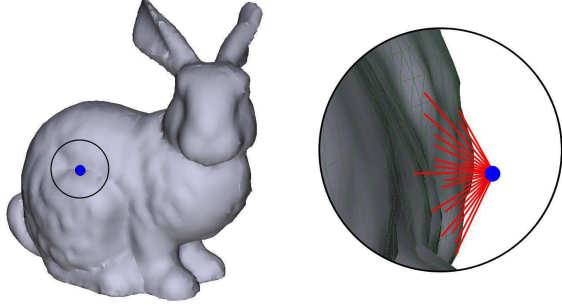
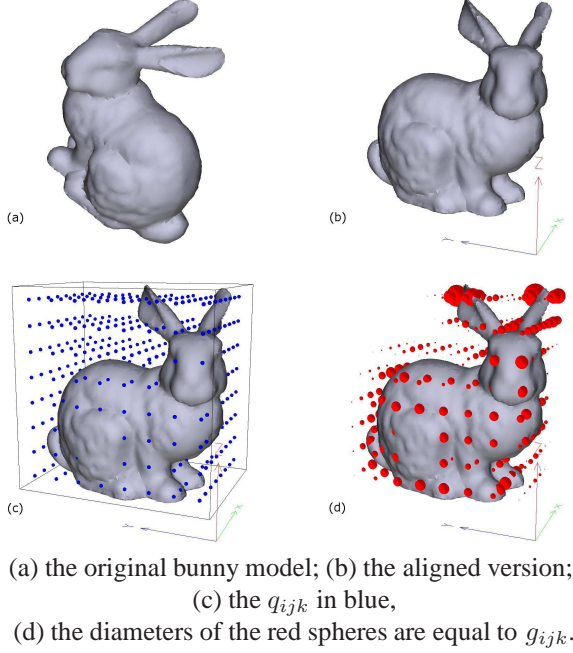


**Fig. 1.** 3DGD on the bunny model

### 2.1.1. Discrete approximation

The 3D Gaussian Descriptor computation is based on an histogram accumulation process, each  $g_{ijk}$  being given by the integral sum of the contributions of the points of  $\mathfrak{S}$  on  $q_{ijk}$ . To compute a discrete approximation of equation 2, we approximate  $\mathfrak{S}$  by a finite set  $E$  of points uniformly distributed on  $\mathfrak{S}$ . Then equation 2 becomes:

$$g_{ijk} = \sum_{\mathbf{p} \in E} e_{ijk}^{\mathbf{p}}. \quad (4)$$

The set of points  $E$  must be appropriately chosen to obtain a robust representation of  $\mathfrak{S}$ . For that purpose, a pseudo-uniform subdivision of each triangular facet  $T_i$ ,  $i = 1 \dots N_T$ , into  $n_i$  triangles  $\{T_i^j\}_{1 \dots n_i}$  having almost the same area is processed. Then the set  $E$  is defined by:

$$E = \bigcup_{i=1}^{N_T} \bigcup_{j=1}^{n_i} \mathbf{g}_i^j, \quad (5)$$

$\mathbf{g}_i^j$  being the centroid of  $T_i^j$ .

The sampling rate  $n_i$  of  $T_i$  is computed using  $n_{min}$ , the minimal number of samples associated to the surface  $\mathfrak{S}$ , i.e.  $n_i = \lceil \frac{A_i}{A} n_{min} \rceil$ .

The 3D model may contain very small faces that won't be subdivided by the previous process. Then, to take into account the variation of facets areas, equation (3) is replaced by:

$$e_{ijk}^{\mathbf{p}} = A_{\mathbf{p}} e^{-d^2(\mathbf{p}, \mathbf{q}_{ijk})/\sigma^2}. \quad (6)$$

$A_{\mathbf{p}}$  being the area of the facet having  $\mathbf{p}$  as centroid.

## 2.2. Computation

A naive computation of  $\mathbf{G} = [g_{ijk}]$  can be done by successively examining the contributions of points  $\mathbf{p}$  of  $E$  in the value  $g_{ijk}$ . This has an expensive cost:  $O(|E|N^3)$ . A study on the Gaussian term and a reordering of the computation will accelerate the whole process.

### 2.2.1. Gaussian term

Let us first examine the contribution of a point  $\mathbf{p}$  in the local description  $g_{ijk}$ . If  $\mathbf{p}$  is in a neighborhood of  $\mathbf{q}_{ijk}$ ,  $e_{ijk}^{\mathbf{p}}$  is strictly positive and  $g_{ijk}$  is incremented.

On the other hand, when  $\mathbf{p}$  is far from  $\mathbf{q}_{ijk}$ ,  $e^{-d^2(\mathbf{p}, \mathbf{q}_{ijk})/\sigma^2}$  is nearly equal to zero ( $e^{-d^2(\mathbf{p}, \mathbf{q}_{ijk})/\sigma^2} < \epsilon$ ,  $\epsilon$  being a very small threshold value). Then  $\mathbf{p}$  does not contribute to the local description around  $\mathbf{q}_{ijk}$ , and  $g_{ijk}$  stays unchanged.

Suppose the threshold  $\epsilon > 0$  fixed and let us consider the neighboring ball  $\mathcal{B}_{ijk} = \{\mathbf{q} \in \mathbb{R}^3 | d(\mathbf{q}, \mathbf{q}_{ijk}) \leq \sigma \sqrt{-\ln(\epsilon)}\}$ . The sampling points  $\mathbf{p}$  of  $E$  which intersect  $\mathcal{B}_{ijk}$  are such that  $e_{ijk}^{\mathbf{p}} \geq \epsilon$  and are the only ones taken into account when computing  $g_{ijk}$  (cf. Figure 1). Thus  $e_{ijk}^{\mathbf{p}}$  can be replaced by:

$$e_{ijk}^{\mathbf{p}} = \delta_{\mathcal{B}_{ijk}}(\mathbf{p}) A_{\mathbf{p}} e^{-d^2(\mathbf{p}, \mathbf{q}_{ijk})/\sigma^2}, \quad (7)$$

$\delta_{\mathcal{B}_{ijk}}$  being the membership function:

$$\delta_{\mathcal{B}_{ijk}}(\mathbf{p}) = \begin{cases} 1 & \text{if } \mathbf{p} \in \mathcal{B}_{ijk}, \\ 0 & \text{if } \mathbf{p} \notin \mathcal{B}_{ijk}, \end{cases} \quad (8)$$

Moreover, when  $\mathbf{p} = (x, y, z)$  belongs to  $\mathcal{B}_{ijk}$ , we have:

$$|x - x_i|^2 + |y - y_j|^2 + |z - z_k|^2 \leq r^2$$

with  $r = \sigma \sqrt{-\ln(\epsilon)}$ , which is done when  $q_{ijk} = (x_i, y_j, z_k)$  satisfies the three inequalities:

$$|x - x_i|^2 \leq r^2,$$

$$|y - y_j|^2 \leq r^2 - |x - x_i|^2,$$

$$|z - z_k|^2 \leq r^2 - |x - x_i|^2 - |y - y_j|^2,$$

Thus, to select the balls that intersect  $\mathbf{p}$ , we compute the lower and upper indices of the  $q_{ijk}$  coordinates, restricting the space of the associated balls  $\mathcal{B}_{ijk}$  containing  $\mathbf{p}$ :

$$i \in \{i^d, \dots, i^f\}, j \in \{j_i^d, \dots, j_i^f\}, k \in \{k_{ij}^d, \dots, k_{ij}^f\}, \text{ with}$$

$$x_{i^f-1} < x + r \leq x_{i^f} \text{ and } x_{i^d} \leq x - r < x_{i^d+1},$$

$$y_{j_i^f-1} < y + \sqrt{r^2 - |x - x_i|^2} \leq y_{j_i^f} \text{ and}$$

$$y_{j_i^d} \leq y - \sqrt{r^2 - |x - x_i|^2} < y_{j_i^d+1},$$

$$z_{k_{ij}^f-1} < z + \sqrt{r^2 - |x - x_i|^2 - |y - y_i|^2} \leq z_{k_{ij}^f} \text{ and}$$

$$z_{k_{ij}^d} \leq z - \sqrt{r^2 - |x - x_i|^2 - |y - y_i|^2} < z_{k_{ij}^d+1}.$$

### 2.2.2. Descriptor normalisation

In equation 6, the facet area has been introduced in the computation of  $e_{ijk}^{\mathbf{p}}$ . There exist 3D shapes having similar local characteristics but with very different facets areas. To limit this skew, we propose to summon the surfaces of the facets associated with points of  $\mathcal{B}_{ijk}$  that contribute to  $g_{ijk}$  and to normalise it with respect to this sum:

$$\mathcal{A}_{ijk} = \sum_{\mathbf{p} \in E'} \delta_{\mathcal{B}_{ijk}}(\mathbf{p}) \mathcal{A}_{\mathbf{p}}, \quad (9)$$

$$g_{ijk} = \frac{1}{\mathcal{A}_{ijk}} \sum_{\mathbf{p} \in E'} e_{ijk}^{\mathbf{p}}.$$

$\delta_{\mathcal{B}_{ijk}}$  being the membership function defined in equation 8.

### 2.2.3. Descriptor computation

Thus, given the set  $E$  of sampling points, the  $g_{ijk}$  are computed by the algorithm of Figure 2.

### 2.3. Similarity measure

To compare two 3D models  $\mathcal{M}_1$  and  $\mathcal{M}_2$  we proceed as follows:

1. Each model is translated to the origin of world coordinate system, scaled such that the average distance is 1 and aligned using either our alignment method [9, 10] or the ‘‘Continuous PCA’’ [8].
2. Two Gaussian descriptors are computed  $\mathbf{G}_1 = [g_{ijk}^1]$  and  $\mathbf{G}_2 = [g_{ijk}^2]$ .
3. The similarity between  $\mathcal{M}_1$  and  $\mathcal{M}_2$  is measured using two different techniques described below.

The first similarity measure  $\Delta$  corresponds to the Euclidean distance in the Gauss coefficients space:

$$\Delta(\mathcal{M}_1, \mathcal{M}_2) = d(\mathbf{G}_1, \mathbf{G}_2), d \text{ being norm } L^1 \text{ or } L^2.$$

### 3D GAUSSIAN DESCRIPTOR( $E, \sigma, \epsilon$ )

$$r = \sigma \sqrt{-\epsilon}$$

**For all**  $i, j, k$  in  $\{0, \dots, N-1\}$

$$g_{ijk} = \mathcal{A}_{ijk} = 0$$

**For all point**  $\mathbf{p}$  of  $E$

compute  $i^d$  and  $i^f$

**For all**  $i$  in  $\{i^d, \dots, i^f\}$

$$d_{x_i}^2 = (x - x_i)^2$$

**if** ( $d_{x_i}^2 \leq r^2$ ) **then**

compute  $j_i^d$  and  $j_i^f$

**for all**  $j$  in  $\{j_i^d, \dots, j_i^f\}$

$$d_{y_j}^2 = (y - y_j)^2$$

**if** ( $d_{x_i}^2 + d_{y_j}^2 \leq r^2$ ) **then**

compute  $k_{ij}^d$  and  $k_{ij}^f$

**for all**  $k$  in  $\{k_{ij}^d, \dots, k_{ij}^f\}$

$\setminus \setminus \mathbf{p}$  belongs to  $\mathcal{B}_{ijk}$   $\setminus \setminus$

$$d_{z_k}^2 = (z - z_k)^2$$

$$d^2(\mathbf{p}, \mathbf{q}_{ijk}) = d_{x_i}^2 + d_{y_j}^2 + d_{z_k}^2$$

$$\mathcal{A}_{ijk} += \mathcal{A}_{\mathbf{p}}$$

$$g_{ijk} += \mathcal{A}_{\mathbf{p}} e^{-d^2(\mathbf{p}, \mathbf{q}_{ijk})/\sigma^2}$$

**For all**  $i, j$  and  $k$  in  $\{0, \dots, N-1\}$

$$g_{ijk} / = \mathcal{A}_{ijk}$$

**Fig. 2.** Algorithm 3D GAUSSIAN DESCRIPTOR

The second one,  $\Delta'$ , is more robust to small variations:

$$\Delta'(\mathcal{M}_1, \mathcal{M}_2) = \sum_{i=0}^{N-1} \sum_{j=0}^{N-1} \sum_{k=0}^{N-1} \min \left\{ \begin{array}{l} |g_{ijk}^1 - g_{ijk}^2|, \\ d_{ijk}(g^1, g^2), \\ d_{ijk}(g^2, g^1) \end{array} \right.$$

$$d_{ijk}(g^p, g^q) = \min |g_{ijk}^p - g_{i'j'k'}^q| \text{ for } |i-i'|+|j-j'|+|k-k'|=1.$$

## 3. RESULTS

We made our tests on the Test Princeton 3D Shape Benchmark database [2] where 907 models are categorized within 92 distinct classes. To compare objectively the retrieval effectiveness of the proposed approaches, we compute Precision-Recall diagrams commonly used in information search (the query is not counted in the answer as in [8]). Four methods AL-3DGA-Dv, AL-3DGA-L1, CPCA-3DGA-L1 and CPCA-VOX-L1 have been tested (cf. Figure 3), where:

- AL or CPCA denote the alignment method used (either CPCA [8] or our alignment method AL [9]),
- The 3D description is our 3D Gaussian descriptor for 3DGA or uses the voxel-based feature vector introduced in Vranic’s thesis [8] for VOX.
- The similarity measure is either  $\Delta$  with  $L_1$  distance for L1 or  $\Delta'$  for Dv.

The precision-recall curves of Figure 3 show that the choices

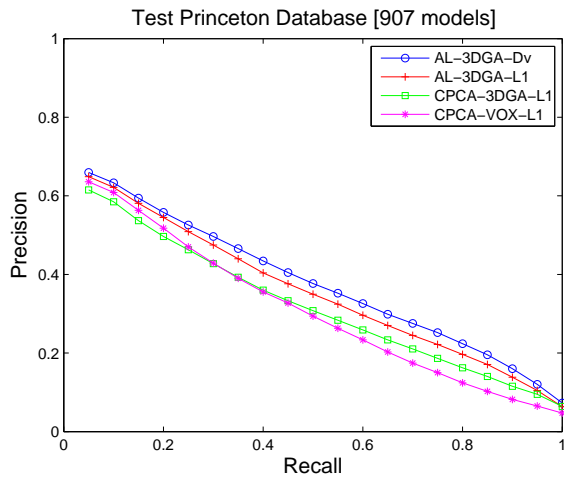


**Fig. 3.** Average precision-recall diagrams on the Test Princeton Database

of our alignment method and of the distance  $\Delta'$  improve the overall retrieval performances. Moreover, the 3D Gaussian descriptor is better than the voxel-based descriptor of Vranic.

#### 4. CONCLUSION

The 3D Gaussian approach presented in this paper computes a compact and rapid global description for 3D shapes. It is adapted to generic shape database as Princeton Shape Benchmark database. It has good retrieval performances for classes of objects having a small variability of shape such as planes, doors or monitors, as illustrated in Figure 4.

Moreover, our method has good results inside the partition-based approaches (cf. the precision recall diagram of Figure 3) and can be retained among global description methods to build a hybrid 3D descriptor as done in [11].

#### 5. REFERENCES

- [1] J.W.H. Tangelder and R.C. Veltkamp, "A survey of content based 3D shape retrieval methods," *Multimedia Tools and Applications*, vol. 39, no. 3, pp. 441–471, Sept. 2008.
- [2] P. Shilane, P. Min, M. Kazhdan, and T. Funkhouser, "The Princeton shape benchmark," in *Shape Modeling and Applications Conference, SMI'2004*, Genova, Italy, June 2004, IEEE, pp. 167–178.
- [3] T. Zaharia and F. Prêteux, "3D versus 2D/3D shape descriptors: A comparative study," in *SPIE Conf. on Image Processing: Algorithms and Systems III - IS & T / SPIE Symposium on Electronic Imaging, Science and Technology '03, San Jose, CA*, Jan. 2004, vol. 5298.

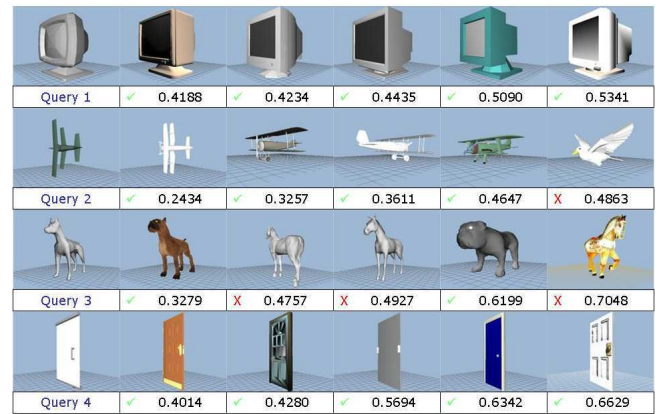


**Fig. 4.** Examples of similarity search. For each query, we show the top 5 objects matched with 3DGD based approach. The similarities between the query models and the retrieved models are given below corresponding images. ✓ and ✗ indicate that the retrieved models belong or don't belong to the query's class, respectively.

- [4] B. Bustos, D. A. Keim, T. Schreck, and D. Vranic, "An experimental comparison of feature-based 3D retrieval methods," in *2nd Int. Symp. on 3D Data Processing, Visualization, and Transmission (3DPVT'04)*, Thessaloniki, Greece, Sept. 2004.
- [5] A. Del Bimbo and P. Pala, "Content-based retrieval of 3D models," *ACM Trans. Multimedia Comput. Commun. Appl.*, vol. 2, no. 1, pp. 20–43, 2006.
- [6] M. Ankerst, G. Kastenmüller, H.-P. Kriegel, and T. Seidl, "3D shape histograms for similarity search and classification in spatial databases," in *6th Int. Symp. on Large Spatial Databases (SSD'99)*, Hong Kong, China, 1999, vol. 1651 of *LNCIS*, pp. 207–226, Springer.
- [7] J.W.H. Tangelder and R.C. Veltkamp, "Polyhedral model retrieval using weighted point sets," Tech. Rep. UU-CS-2002-019, Universiteit Utrecht, 2002.
- [8] D.V. Vranic, *3D Model Retrieval*, Ph.D. thesis, University of Leipzig, 2004.
- [9] M. Chaouch and A. Verroust-Blondet, "A novel method for alignment of 3D models," in *Shape Modeling and Applications Conference, SMI'2008*, June 2008, pp. 187–195.
- [10] M. Chaouch and A. Verroust-Blondet, "Alignment of 3D models," *Graphical Models*, 2009, accepted for publication.
- [11] P. Papadakis, I. Pratikakis, T. Theoharis, G. Passalis, and S. Perantonis, "3D object retrieval using an efficient and compact hybrid shape descriptor," in *Eurographics 2008 Workshop on 3D Object Retrieval*, Crete, Greece, Apr. 2008.